DOING PHYSICS WITH PYTHON

COMPUTATIONAL OPTICS

RS1 DIFFRACTION INTEGRAL:

FOCUSED BEAM

ANNULAR APERTURE

Ian Cooper

Please email me any corrections, comments, suggestions or additions: **matlabvisualphysics@gmail.com**

DOWNLOAD DIRECTORIES FOR PYTHON CODE

Google drive

GitHub

emRSFBXY.py

Calculation of the radiant flux density (irradiance) in a plane perpendicular to the optical axis for the radiant flux of convergent beam emitted from a circular aperture.

emFBZX.py

Calculation of the irradiance in the meridional (XZ plane) for the radiant flux of convergent beam emitted from a circular aperture.

emRSFBZ.py

Calculation of the radiant flux density (irradiance) along the optical axis for the radiant flux of convergent beams emitted from a circular aperture.

Warning: The results of the integration may look OK but they may not be accurate if you have used insufficient number of partitions for the aperture space and observation space. It is best to check the convergence of the results as the number partitions is increased. Note: as the number of partitions increases, the calculation time **rapidly** increases.

It is necessary to modify the Python Codes and comment or uncomment lines of code to run the simulations with different input and output parameters, and for different aperture functions.

Link: essential reference

RS1 diffraction integral: Focused beam from a circular aperture

INTRODUCTION

A focused beam with an annular aperture at the front of a lens, can create a doughnut-shaped beam or a non-diffracting beam with an extended depth of focus, which means the beam's intensity pattern doesn't change much over a larger distance, extending the depth of field.

The extended depth of focus makes annular apertures useful for laser remote sensing, allowing for measurements over longer distances with better accuracy. The ability to transmit light over longer distances without significant beam spreading is beneficial for free-space laser communication.

Annular apertures are used in microscopy to improve image quality and resolution, as well as enhance depth of focus.

Ring patterns generated with annular apertures can be used for high-power laser drilling applications.

Annular apertures can also be used in applications requiring non-diffracting beams, such as optical traps, and in optical systems with annular mirrors.

The diffraction pattern from an annular aperture is computed by integrating the RS1 Diffraction integral using a [2D] form of Simpson's rule.

SIMULATIONS

The aperture electric field $E_Q\left(x_{Q,}y_Q,0\right)$ is calculated over a rectangular grid of n_Q x n_Q grid points. The electric field E_Q is non-zero in the annulus of the circular aperture. The electric E_Q in the plane of the aperture field corresponds to a spherical wave converging to the focal point $\left(x_S=0,y_S=0,z_S=f\right)$.

The radius of the circular aperture is a and the radius of the inner of the blocked centre part of the aperture is a_I where

$$a_I = q\,a \qquad 0 < q \le 1$$

Default values used in the simulations are displayed in the Console Window.

wavelength wL = 500 nm
aperture outside radius a = 10.000 mm
Source
xS = 0 m yS = 0 m zS = 0.200 m
Focal length f = 0.200 m
Numerical aperture NA = 0.0499
Fresnel number NF = 1000

The simulations are summarized below for inner radius a_I where q = 1.0 (circular aperture), 0.5, 0.85, and 0.95.

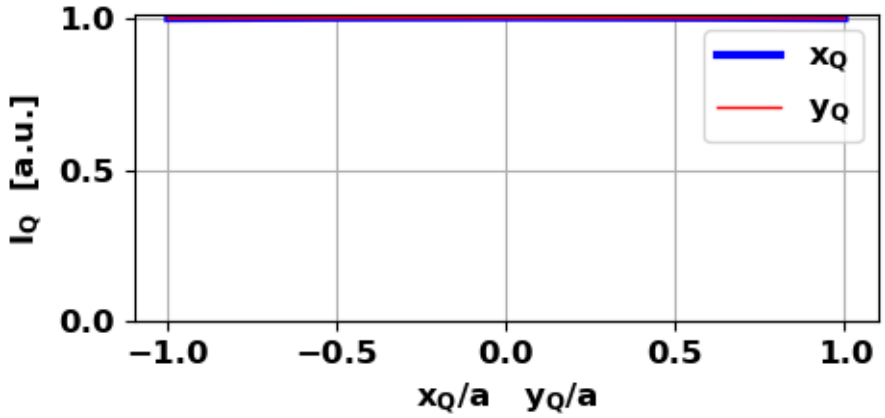

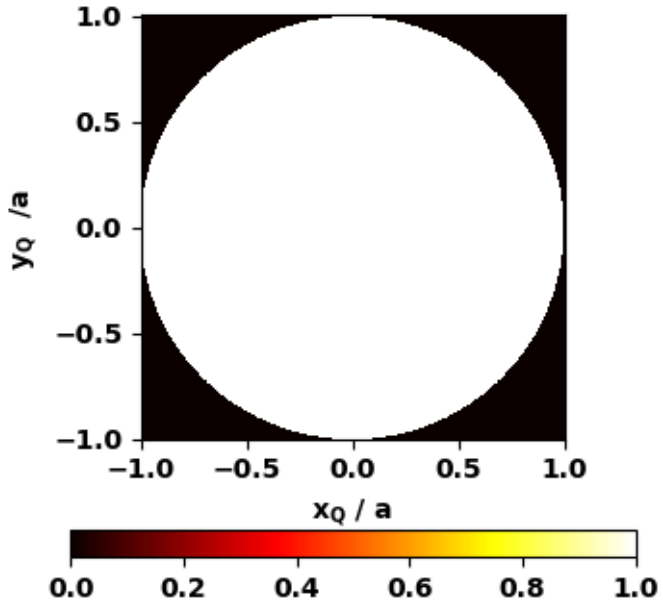

Fig.1A. Full circular aperture: $a_I = 1.00\,a$

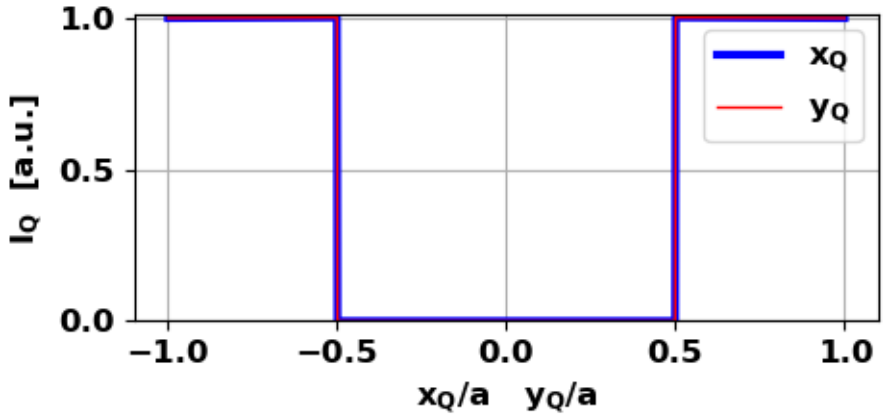

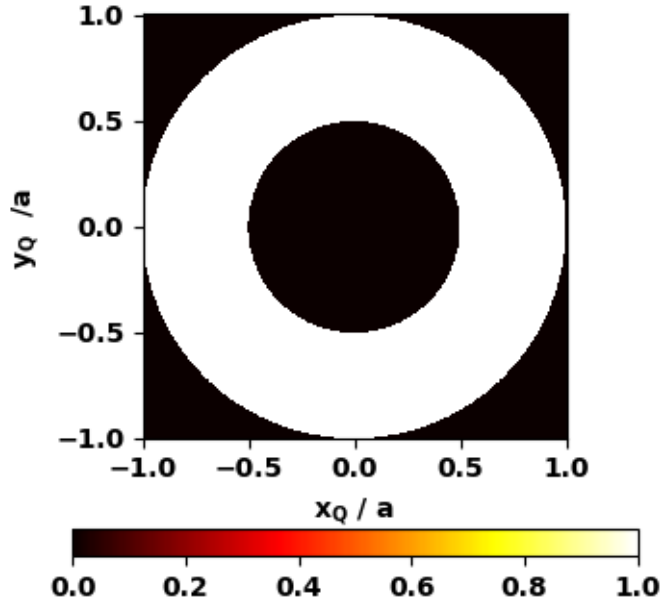

Fig. 1B. Annular aperture: $a_I = 0.50\,a$

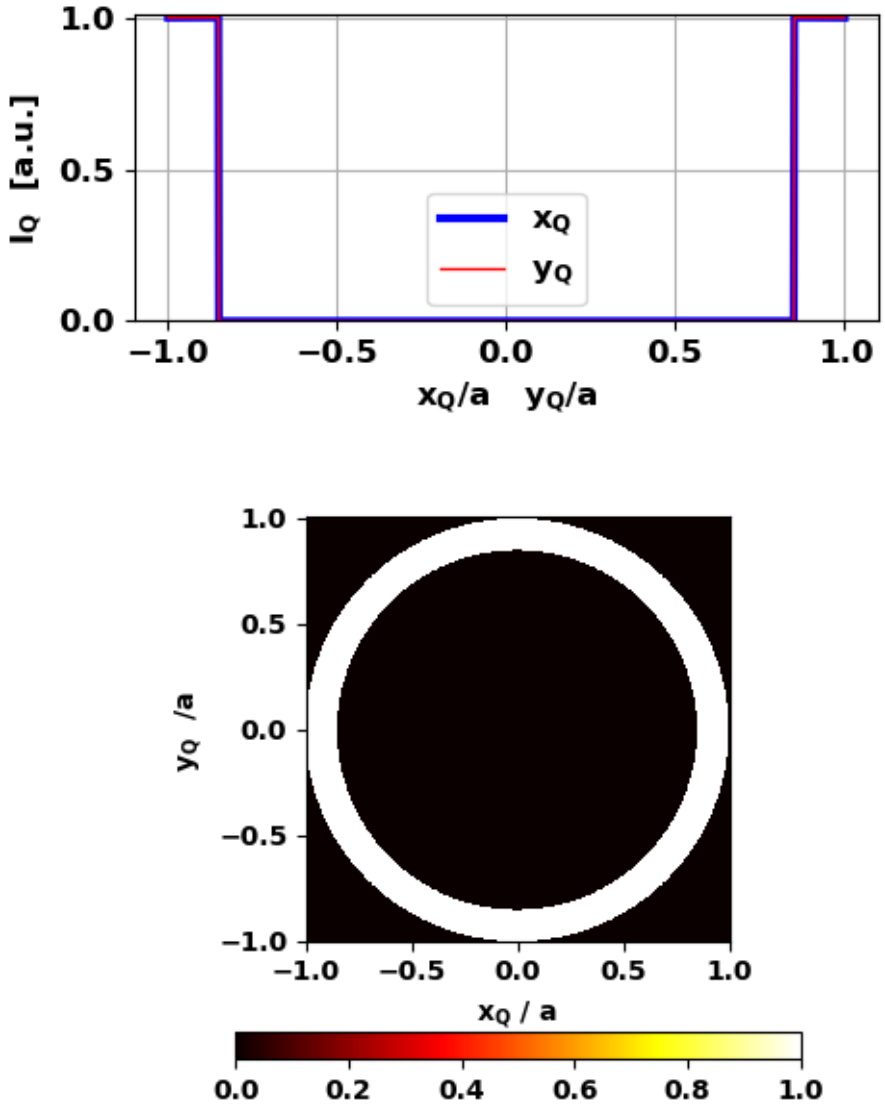

Fig. 1C. Annular aperture: $a_I = 0.85\,a$

Axial irradiance along the optical axis (Z axis)

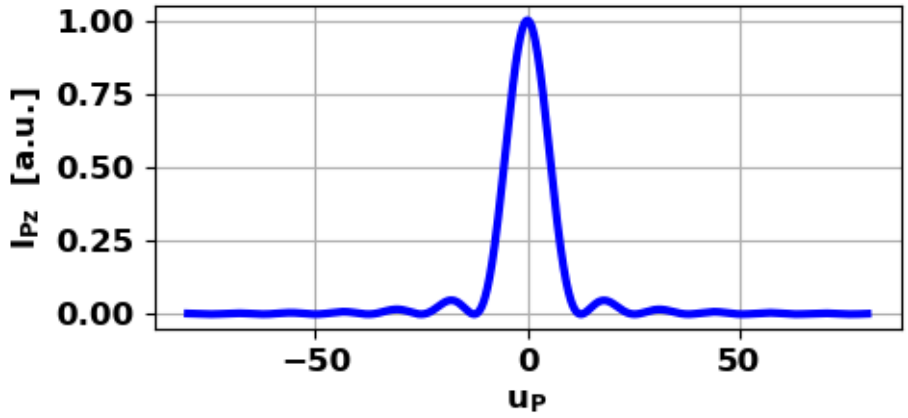

Fig. 2A. Axial irradiance: Full circular aperture: $a_I = 1.00\,a$

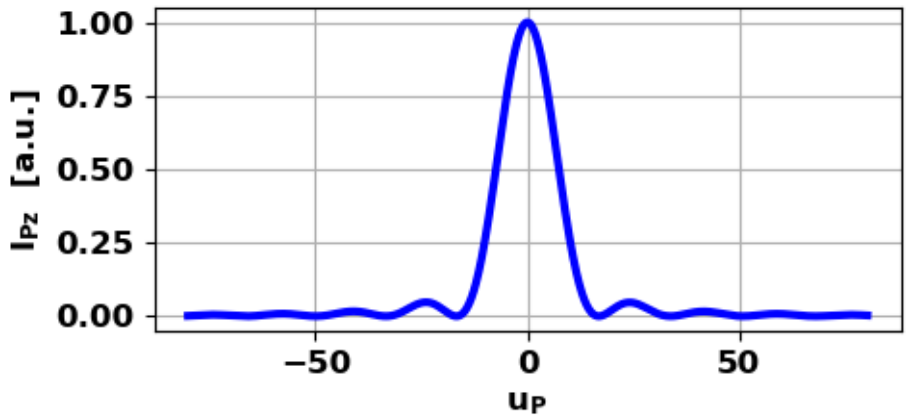

Fig. 2B. Axial irradiance: Annular aperture: $a_I = 0.50\,a$

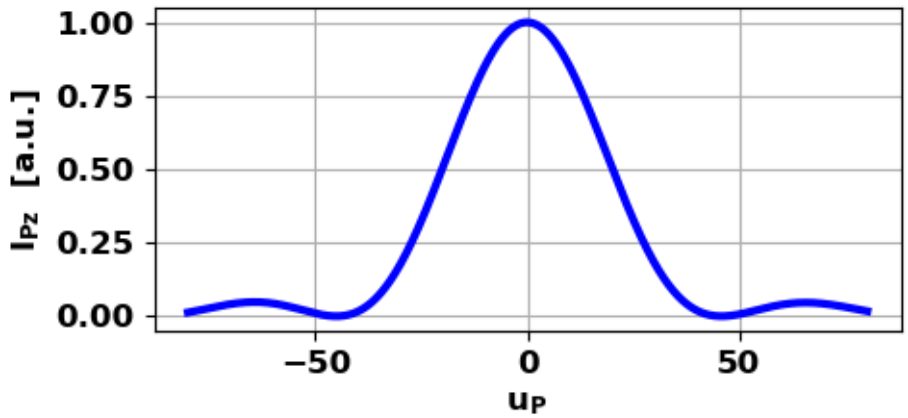

Fig. 2C. Axial irradiance: Annular aperture: $a_I = 0.85\,a$

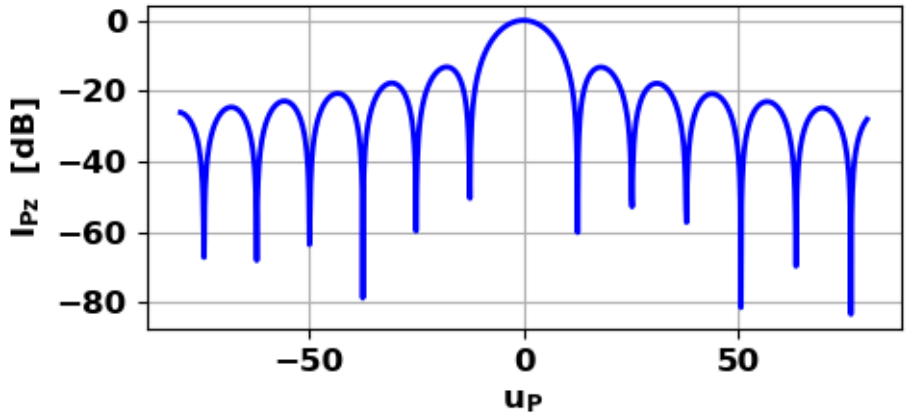

Fig. 3A. Axial irradiance: Full circular aperture: $a_I = 1.00\,a$

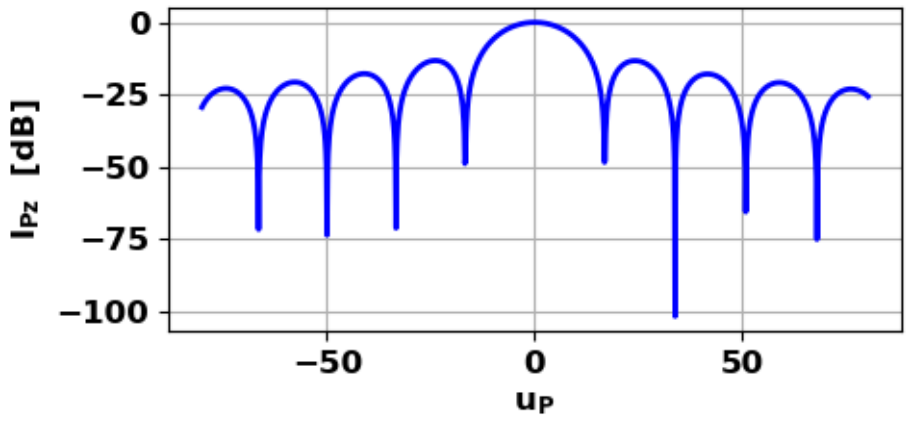

Fig. 3B. Axial irradiance: Annular aperture: $a_I = 0.50\,a$

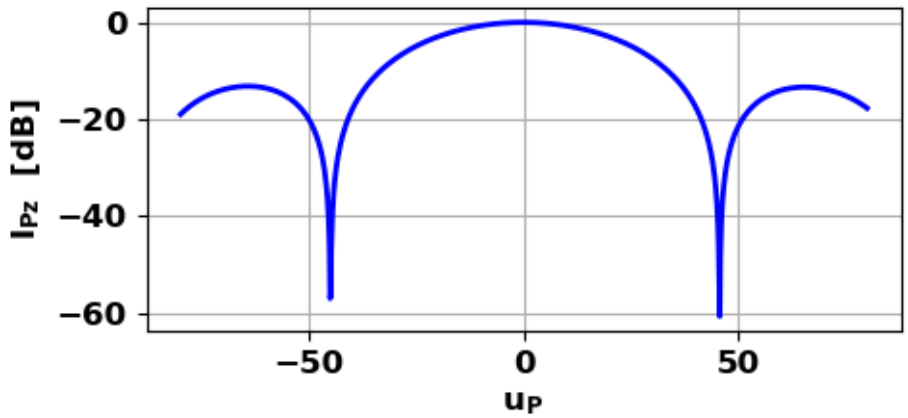

Fig. 3C. Axial irradiance: Annular aperture: $a_I = 0.85\,a$

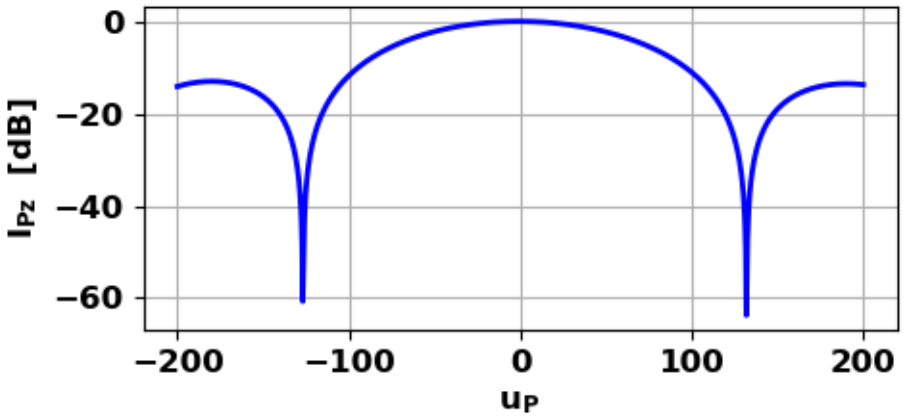

Fig. 3D. Axial irradiance: Annular aperture: $a_I = 0.95a$

Table 1. Axial irradiance minima u_P locations (error = ± 0.07).

Error in position of u_P values due to discrete grid.

$a_I = 1.00a$	12.63	25.34	38.05	50.76	63.61	76.45
$a_I = 0.50a$	16.78	33..77	50.76	67.89		
$a_I = 0.85a$	45.81					
$a_I = 0.95a$	132					

The plots in figures 2 and 3, and the location of the minima given in Table 1 for the irradiance patterns, clearly shows the depth of focus (width of the axial peak) increase as the width of the annulus becomes narrower. The light distribution near the focus of an annular lens shows that the intensity variation along the optic axis is stretched as the central obstruction is increased. In the limit, as the width of the annulus becomes very small, the intensity along the axis becomes more constant.

Irradiance in the XY focal plane

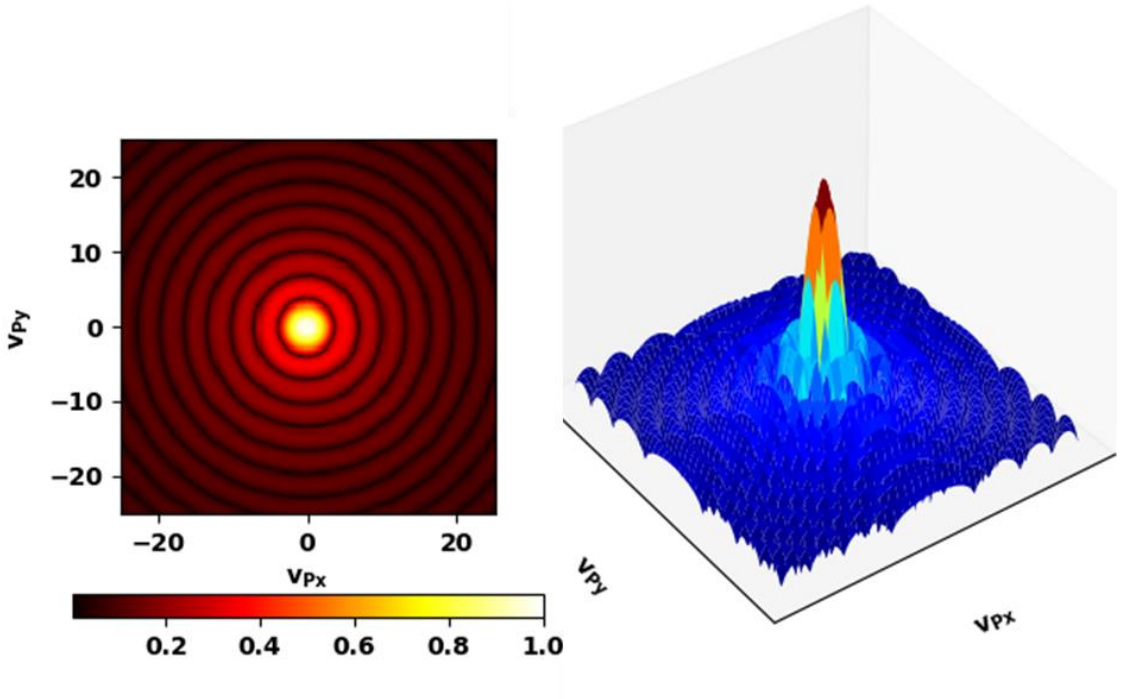

Fig. 4A. Radial irradiance: Full circular aperture: $a_I = 1.00\,a$

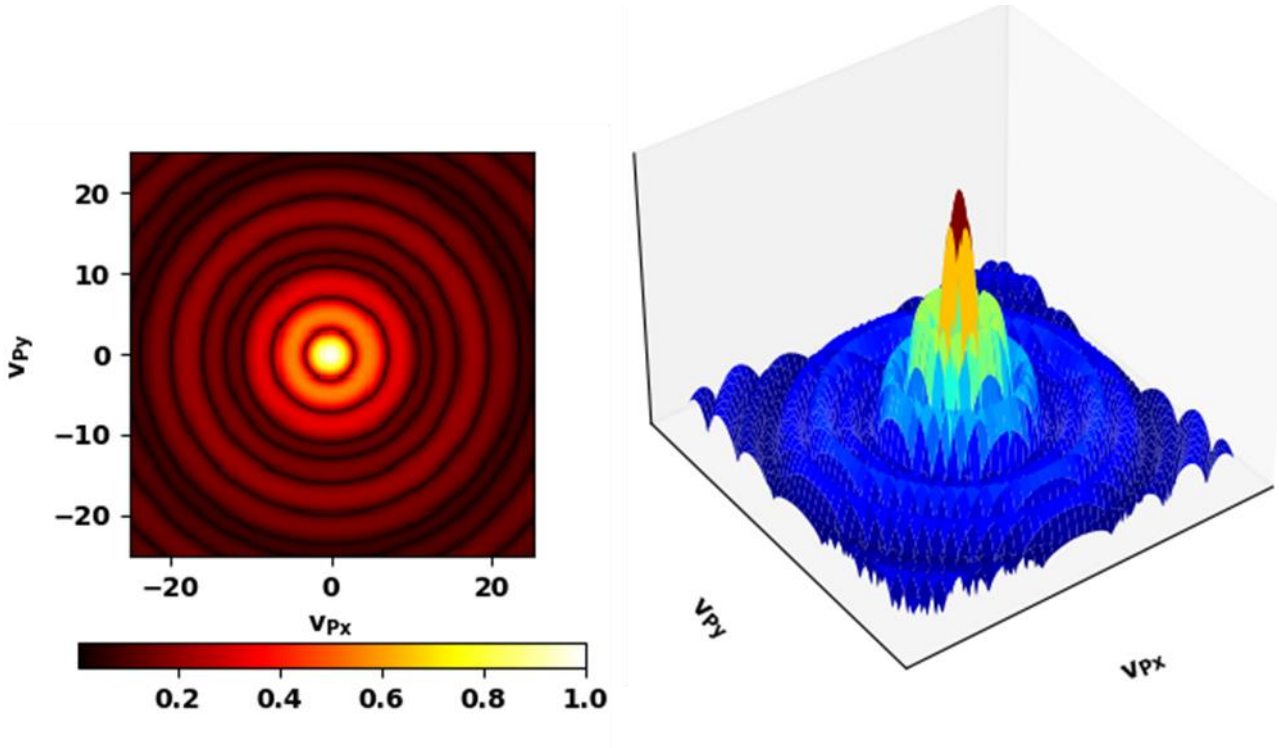

Fig. 4B. Radial irradiance: Annular aperture: $a_I = 0.50\,a$

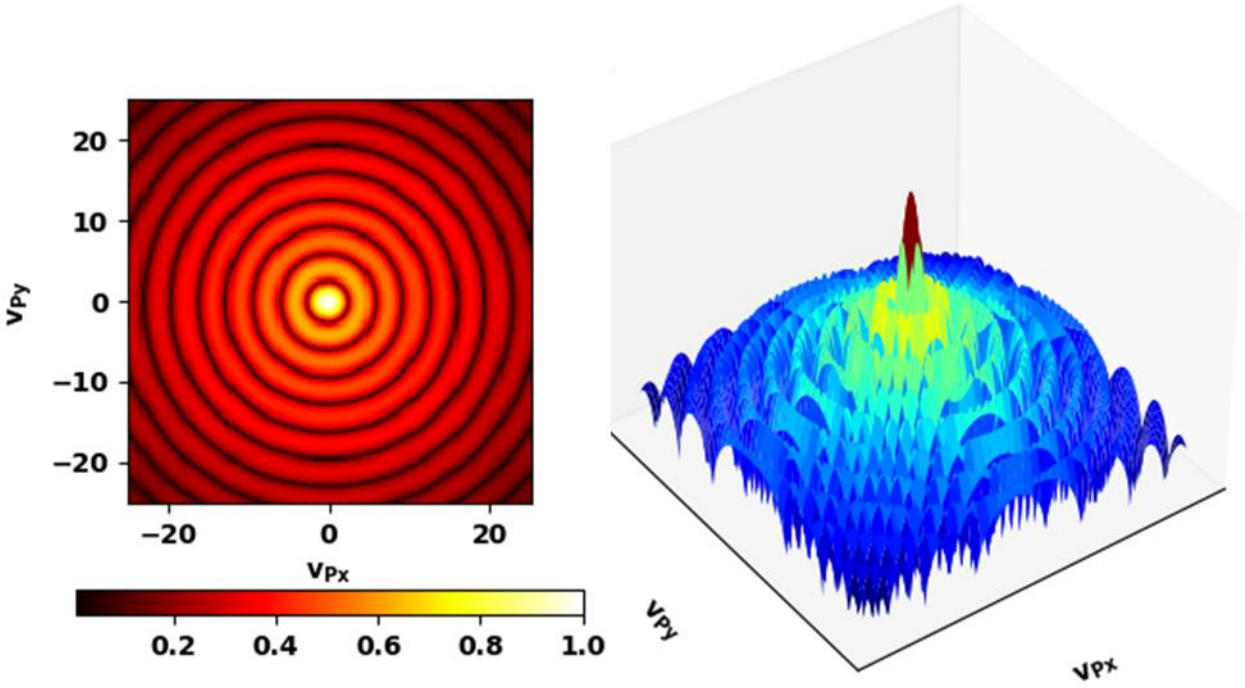

Fig. 4C. Radial irradiance: Annular aperture: $a_I = 0.85\,a$

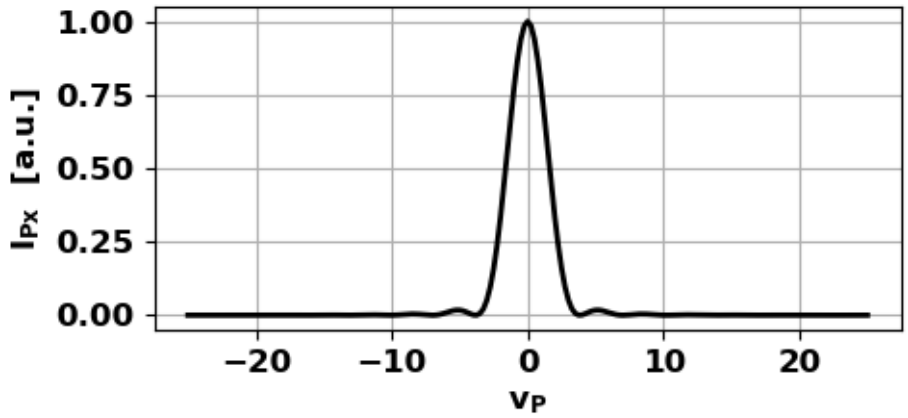

Fig. 5A. Radial irradiance: Full circular aperture: $a_I = 1.00\,a$

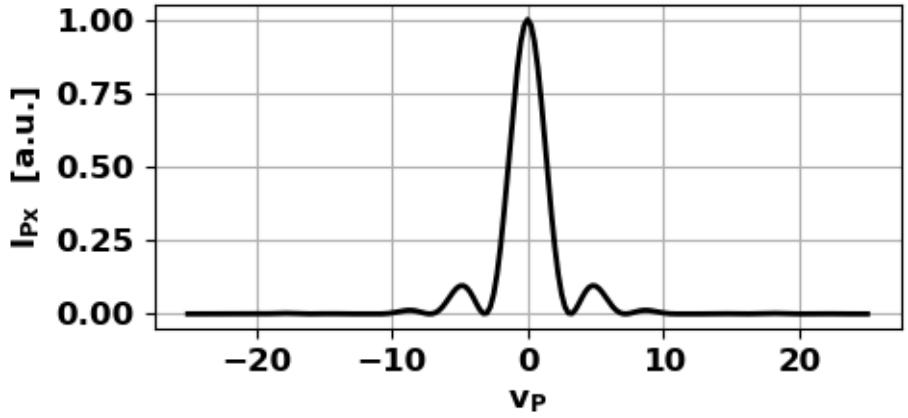

Fig. 5B. Radial irradiance: Annular aperture: $a_I = 0.50\,a$

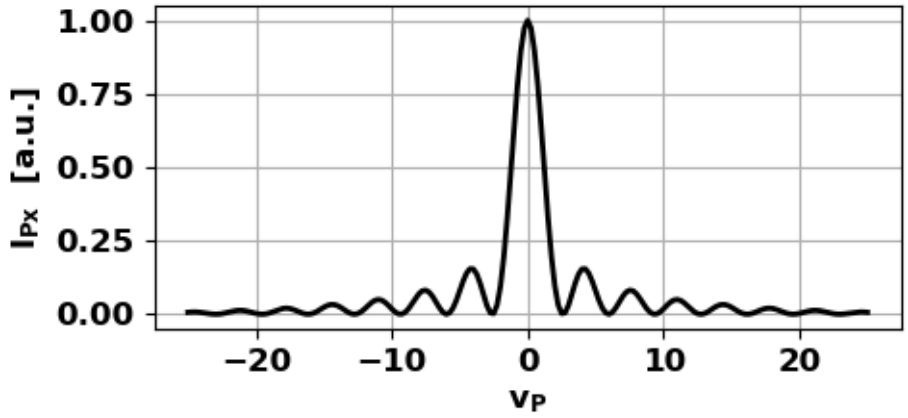

Fig. 5C. Radial irradiance: Annular aperture: $a_I = 0.85\,a$

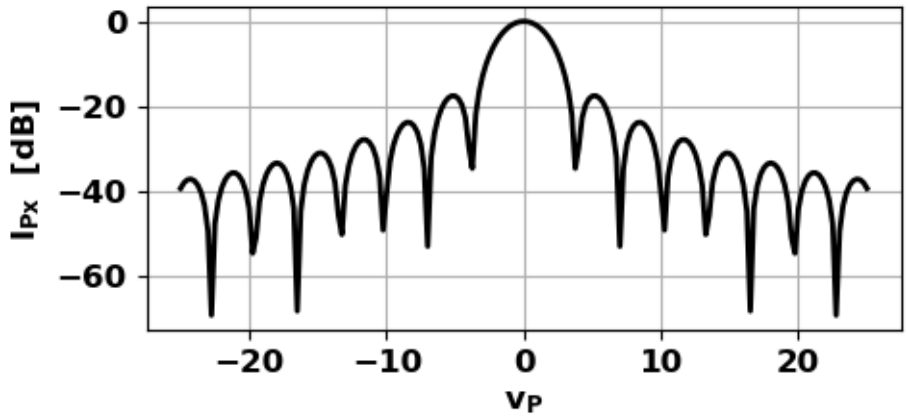

Fig. 6A. Radial irradiance: Full circular aperture: $a_I = 1.00\,a$

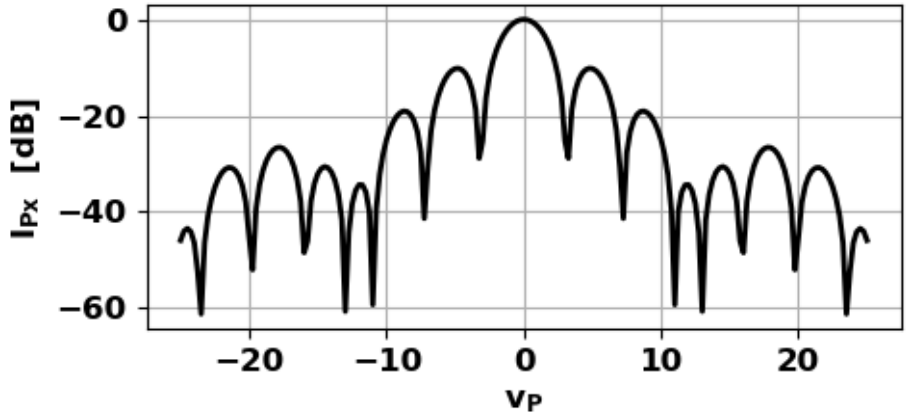

Fig. 6B. Annular aperture: $a_I = 0.50\,a$

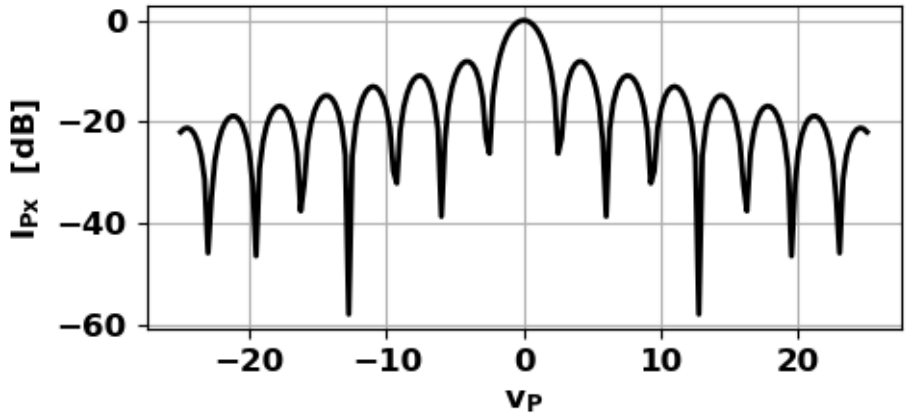

Fig. 6C. Radial irradiance: Annular aperture: $a_I = 0.85\,a$

Table 2. Radial irradiance minima v_P locations (error = ± 0.1).

Error in position of v_P values due to discrete grid.

$a_I = 1.00\,a$	3.8	7.0	10.3	13.3	19.8	22.8
$a_I = 0.85\,a$	3.3	7.3	11.0	13.0	16.0	19.8
$a_I = 0.50\,a$	2.5	6.0	9.3	16.3	19.5	23

The focused beams for all three apertures show a distinctive ring structure in the XY focal plane. The narrow aperture $a_I = 0.85\,a$ has pronounced dark and bright rings with a narrow peak in the irradiance at the focal point.

Irradiance in an XY plane near the focal plane

The irradiance in the XY plane

$$\left(u_P = 45.56 \quad z_P = 0.2014502934206934\right)$$

for the aperture $a_I = 0.85\,a$. This corresponds to an axial minimum in the axial irradiance as shown in figure 3C.

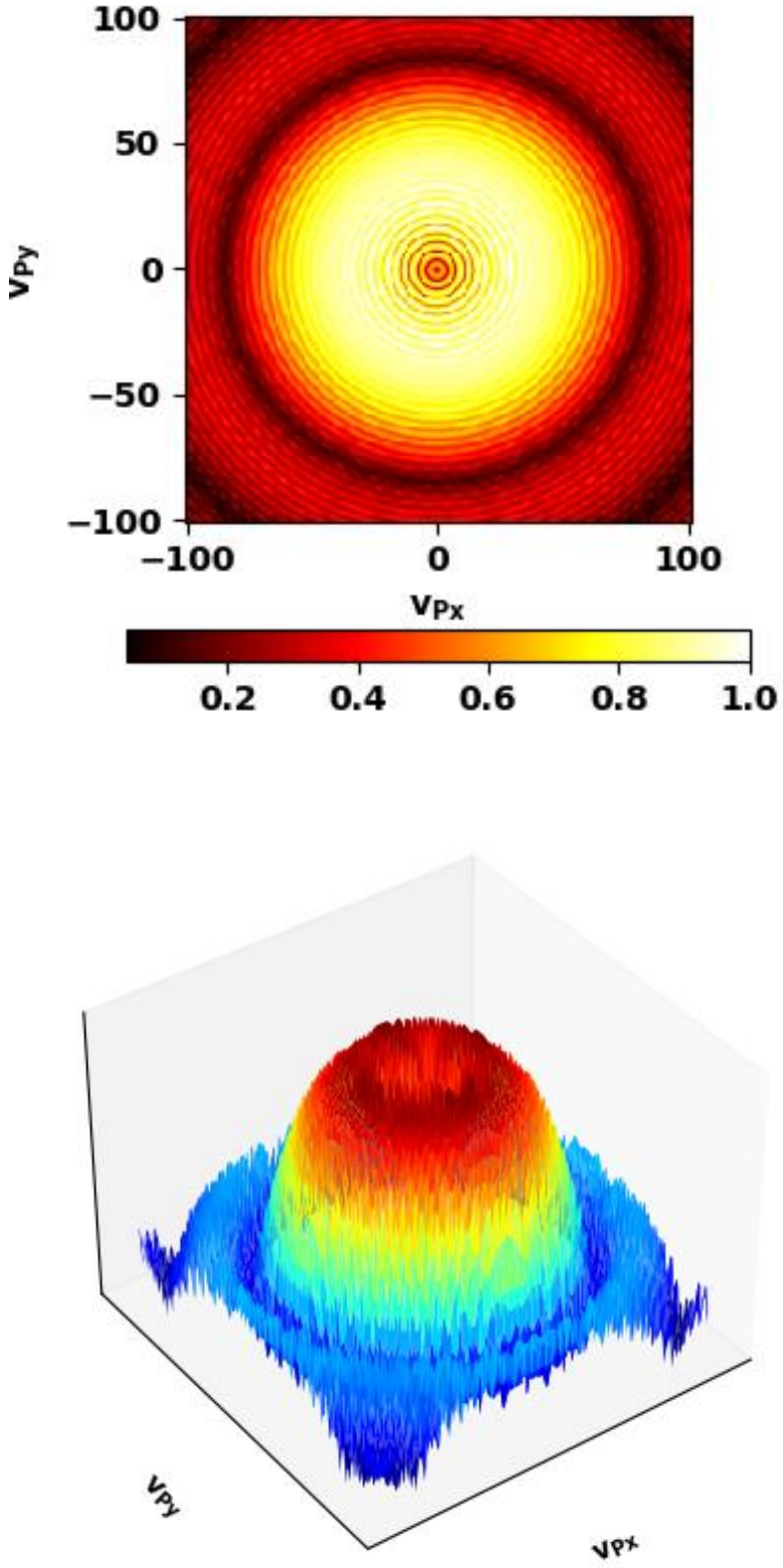

Fig. 7. [2D] and [3D] views of the irradiance the XY plane near the focal plane.

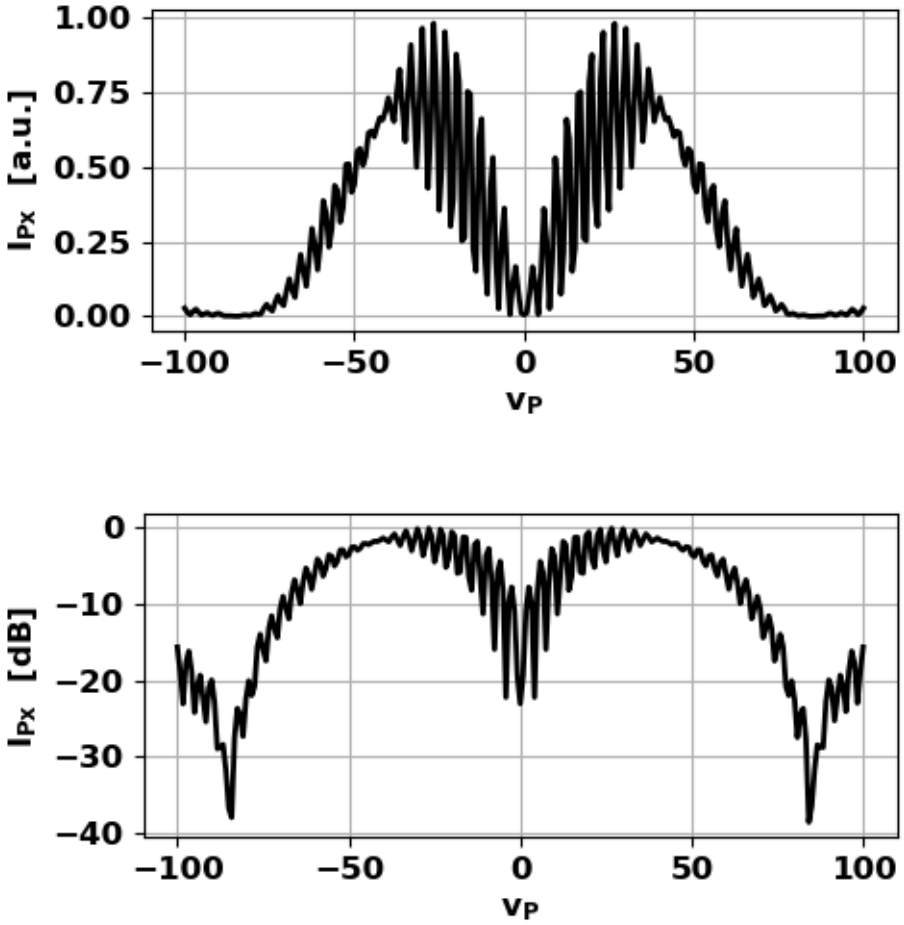

Fig. 8. The radial irradiance the XY plane near the focal plane.

There is a very complex ring structure for this non-focal XY plane with a dark centre in the irradiance pattern. The electric field in the plane of the aperture is circular symmetric and therefore, the irradiance distribution in any XY plane must also be circularly symmetric.

Irradiance in the meridional ZX plane

Figure 9 shows the irradiance pattern in the meridional ZX plane in the focal region for the annular aperture $a_I = 0.85a$.

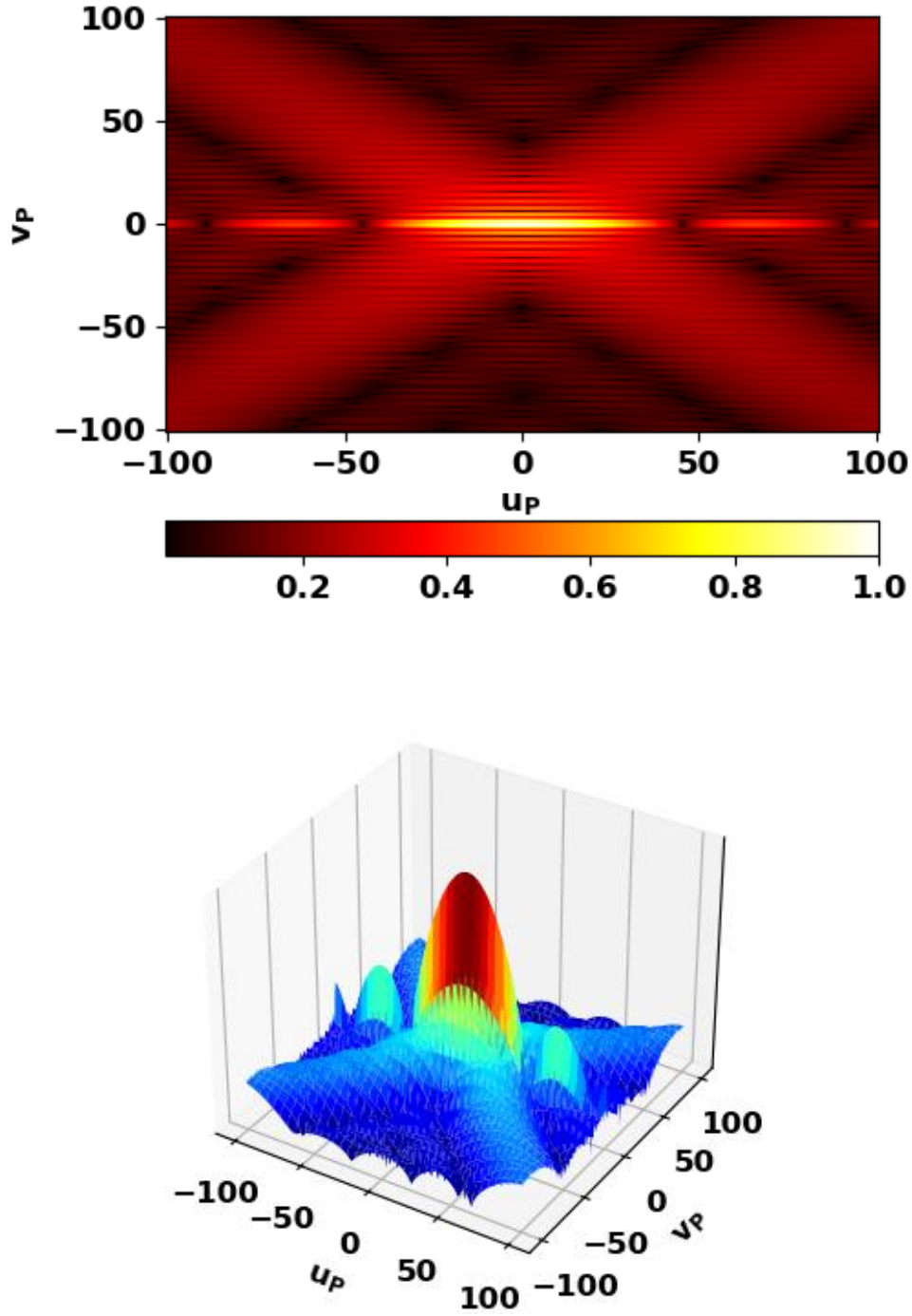

Fig. 9. The irradiance pattern in the meridional ZX plane in the focal region for the annular aperture $a_I = 0.85a$.